

Statistical Design of Chaotic Waveforms with Enhanced Targeting Capabilities

Huanan Li*, Suwun Suwunnarat*, Tsampikos Kottos
Physics Department, Wesleyan University, Middletown CT-06459, USA
(Dated: September 21, 2022)

We develop a statistical theory of waveform shaping of incident waves that aim to efficiently deliver energy at weakly lossy targets which are embedded inside chaotic enclosures. Our approach utilizes the universal features of chaotic scattering – thus minimizing the use of information related to the exact characteristics of the chaotic enclosure. The proposed theory applies equally well to systems with and without time-reversal symmetry.

PACS numbers: Valid PACS appear here

The prospect of utilizing waveform shaping of incident acoustic or electromagnetic radiation in order to efficiently direct energy to focal points, placed inside chaotic (or disordered) enclosures, has been intensely pursued during the last few years [1]. The excitement for this line of research is twofold: On the fundamental side the interesting question is to identify schemes that will allow us to utilize multiple scattering events in complex media like disordered structures or chaotic reverberation cavities in order to overcome the diffraction limit [2–9]. A successful outcome can revolutionize many applications of wave focusing in complex media, including imaging techniques [10–13] medical therapies [14], outdoor or indoor wireless communications [15] and electromagnetic warfare [16].

In this endeavor, the time reversal (TR) and wave front shaping (WFS) are among the most promising wave-focusing schemes with impressive experimental demonstrations in a range of frequencies (see review [1]). Disregarding subtle details, it was shown that the wave focusing process is benefited from the multiple scattering events and reverberation occurring during propagation inside a complex medium [1, 3, 17, 18]. These two methods are complementary in the sense that TR is a broadband approach which results in spatiotemporal focusing of incident waves while WFS is mainly a monochromatic concept which results in maxima of deposited energy at desired foci. Both methods, however, are requiring a time-reversal invariance of the propagation medium—a condition that can be violated either because of inherent losses or because of some external magnetic field. Moreover, they are not addressing the fact that in typical circumstances, where the targets are inside complicated enclosures, the scattering fields demonstrate an extreme sensitivity to the exact configuration of the enclosure, its coupling to the interrogating antennas, the operating frequency etc. Thus, in many practical applications, the design of a waveform with 100% focusing efficiency (for a *specific* configuration of an adiabatically varying

enclosure) is unfortunately irrelevant.

At the same time, there are well developed statistical methods, applicable both in the frame of electrodynamics [19, 20] and acoustics [21–23], whose central theme is the statistical description of wave interferences at any position inside a complex enclosure [24, 25]. The guiding viewpoint of this school of thought is that the (adiabatic) changes of the enclosure render any attempt to describe transport characteristics for a specific "replica" of the system meaningless. Thus, the statistical description constitutes the only meaningful approach for the scattering properties of chaotic enclosures. Obviously this approach does not provide any recipe for the realization of incident waveforms that will lead to foci (hot-spots) inside a complicated enclosure.

In this paper we develop a *statistical* approach for the design of Waveforms with Enhanced Targeted Capabilities (WETACs), that have high probability to deliver large amount of their carrying energy at weakly lossy targets which are placed inside complex enclosures. Our scheme distributes the injected energy carried by a WETAC over multiple channels and utilizes the features of chaotic scattering as they are quantified by the so-called Ericson parameter. The design of WETACs requires a *minimal* information about the enclosure: the loss-strength (conductivity) of the target (with some tolerance); the eigenfrequencies and the eigemode amplitudes of the isolated cavity at the positions of the interrogating antennas and at the target(s). While most of these informations are experimentally accessible via reflection measurements, the field amplitude at the position of the target might not be easily measured. The additional assumption that the latter is given by the ergodic limit of field intensities for chaotic systems is proven successful, particularly for the case of multiple lossy targets. Finally we find that the WETAC algorithms are applicable for systems with and without TR invariance.

Modeling Absorption in Complex Enclosures – A chaotic enclosure is typically modeled by an ensemble of $N \times N$ random matrices H_0 with an appropriate symmetry: in the case that the isolated cavity is TR invariant, H_0 is taken from a Gaussian Orthogonal Ensemble (GOE), while in the case where the TR-symmetry is

*These two authors contributed equally. HL performed the theoretical analysis and SS the numerical analysis

violated it is taken from a Gaussian Unitary Ensemble (GUE) [24, 25]. When (multiple) localized, weakly lossy target(s) with loss-strength γ_d are present, the system is described by the Hamiltonian:

$$H(\{\gamma_d\}) = H_0 - i\Gamma_0; \quad \Gamma_0 = \sum_d \gamma_d |e_d\rangle \langle e_d|, \quad (1)$$

where $\{|e_l\rangle\}$ is the basis where H_0 is written and $d = 1, \dots, N_d$ indicates the lossy target index. We shall assume below that all targets have the same losses i.e. $\gamma_d = \gamma$.

We turn the isolated cavity to a scattering set-up by coupling it with M semi-infinite single-mode leads. The leads feature one-dimensional tight-binding dispersion $E(k) = 2t_L \cos k$ where $k \in [-\pi, \pi]$. The coupling of the cavity with the leads is controlled by the $N \times M$ matrix W with elements $W_{lm} = w\delta_{lm}$ (w is the coupling strength).

The object that characterizes the scattering process of an incident monochromatic wave with energy $E(k)$ (where $k \in (0, \pi]$) is the $M \times M$ scattering matrix $S(k, \gamma)$

$$S(k, \gamma) = -\hat{1} + 2i \frac{\sin k}{t_L} W^T \frac{1}{H_{eff}(k, \gamma) - E(k)} W, \quad (2)$$

where $\hat{1}$ is the $M \times M$ identity matrix and H_{eff}

$$H_{eff}(k, \gamma) = H(\gamma) + \frac{e^{ik}}{t_L} W W^T \quad (3)$$

is an effective Hamiltonian that describes the cavity in the presence of radiative and Ohmic losses.

In the absence of any losses, the scattering matrix is unitary i.e. $S^\dagger(k, \gamma=0)S(k, \gamma=0) = 1$. However when $\gamma \neq 0$, the scattering matrix is sub-unitary and one can define an absorption operator $\mathcal{A} \equiv 1 - S^\dagger S = \mathcal{A}^\dagger$. Using Eq. (2) we get

$$\mathcal{A}(k, \gamma) = -4\gamma \frac{\sin k}{t_L} \sum_d |u_d\rangle \langle u_d|, \quad |u_d\rangle = W^T G |e_d\rangle \quad (4)$$

where $G(k, \gamma) = [H_{eff}^\dagger(k, \gamma) - E(k)]^{-1}$.

The absorbance associated with an incident waveform $|\mathcal{I}\rangle$ is defined as

$$\alpha(k, \gamma) \equiv \frac{\langle \mathcal{I} | \mathcal{A}(k, \gamma) | \mathcal{I} \rangle}{\langle \mathcal{I} | \mathcal{I} \rangle} \in [0, 1] \quad (5)$$

An $\alpha = 1$ indicates that the energy carried by the incident waveform is completely absorbed by the target(s). The opposite limit of $\alpha = 0$ corresponds to an incident waveform that "lost" completely the lossy target(s) and has been either transmitted or (and) reflected by the cavity. Below, we shall use α as a measure of success of a designed waveform to deliver its energy to a lossy target.

Perfect Waveforms –A perfect waveform (PW) corresponds to an incoming wave whose energy is completely

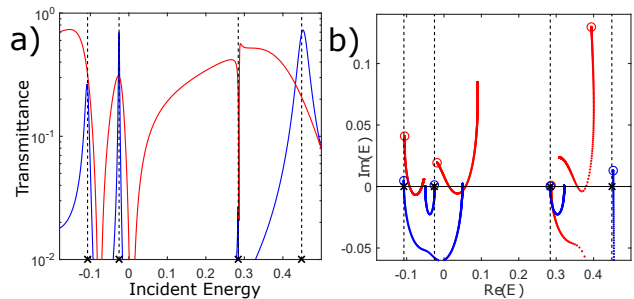


FIG. 1: (color online) (a) The transmittance versus energy for a GOE cavity with one loss target of loss-strength $\gamma = 0.01$. (b) The parametric evolution of complex zeros of the secular equation Eq. (6) in the complex energy plane, as the loss-strength γ increases. In both cases the GOE matrix H_0 has dimensionality $N = 15$, the number of leads is $M = 2$ and the coupling constant of the leads is $t_L = -1$. Blue (red) lines indicate a system with a coupling constant between the leads and the cavity which is $w = -0.2$ ($w = -1$), with a corresponding Ericson parameter $\mathcal{E} \approx 0.03$ ($\mathcal{E} \approx 1.4$) indicating isolated (overlapping) resonances. The complex zeros for $\gamma = 0$ are indicated with open blue/red circles for each case respectively. Black crosses indicate the position of the eigenenergies $E_n^{(0)}$ of the isolated Hamiltonian H_0 .

absorbed by the lossy target(s). The PW $|\mathcal{I}_{PW}\rangle$ is an eigenvector $|\alpha(k_{PW}, \gamma)\rangle$ of $\mathcal{A}(k_{PW}, \gamma)$ with a corresponding eigenvalue $\alpha(k_{PW}, \gamma) = 1$. This condition defines the *real-valued* wavevector k_{PW} . The reality of the wavevector is a physical requirement and it is associated with the fact that, in order to transport energy, the input signal has to be a propagating wave. It deserves to point out that PWs have recently attracted a lot of attention in the framework of optics where they have been identified as the time-reversed of a lasing mode [26, 27]. While these studies are restricted to integrable cavities with TR-symmetry, PWs can also emerge in chaotic systems with or without TR-symmetry [28, 29].

It is straightforward to show that, for a fixed γ , k_{PW} are the *real* zeros (if exist) of the secular equation $\det[S(k, \gamma)] = 0$. Using Eq. (2) one can rewrite the secular equation in terms of the effective Hamiltonian Eq. (3) as [28, 29]

$$\zeta(k, \gamma) \equiv \det(H_{eff}(-k, \gamma) - E(k)) = 0. \quad (6)$$

Note that, for a fixed γ , the secular equation $\zeta(k_n, \gamma) = 0$ has in general multiple complex zeros k_n .

Characterization of chaotic PW based on Ericson Parameter –The scattering properties of a chaotic cavity depend crucially on the way that the system is coupled to the leads. In the case of weak coupling, the scattering matrix exhibit fluctuations on the level of the mean level spacing Δ of the corresponding isolated system [25]. Furthermore, the transmittance consists of resonances that demonstrate narrow linewidths Γ_n which is typically

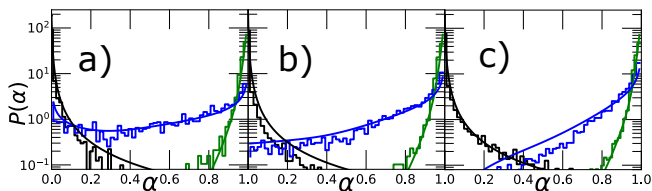


FIG. 2: (color online) Numerical (staircase lines) and theoretical (smooth lines) distribution of absorbances $\mathcal{P}(\alpha)$ for a chaotic cavity with (a) one; (b) two and; (c) four lossy targets. Blue (green) lines are associated to WETAC (ergodic WETAC) incident waveforms. Black lines are associated with an ensemble of $|\mathcal{I}_R\rangle$ incident waveforms. In all cases $M = 2, t_L = -1, w = -0.3$ (corresponding to $\mathcal{E} \approx 0.06$). The dimensionality of H_0 is $N = 15$ while $\bar{\gamma} = 0.01$ and $\eta = 0.35$.

smaller than Δ , see blue line in Fig. 1a. In the opposite limit of strong coupling, the scattering matrix elements develop universal fluctuations due to interference effects between multiple overlapping resonances [25]. Specifically, the scattering amplitudes and transmittances can be represented by a sum of many overlapping resonances, see red line in Fig. 1a.

The distinction between these two qualitative different scattering domains is typically described by the so-called Ericson parameter \mathcal{E} which is defined as the ratio of the mean resonance width $\langle\Gamma\rangle$ to the mean level spacing Δ of the energy levels of the corresponding isolated cavity i.e. $\mathcal{E} = \langle\Gamma\rangle/\Delta$. When $\mathcal{E} \ll 1$ the resonances are well isolated from one another while in the opposite case we have strongly overlapping resonances.

It turns out that the Ericson parameter controls the nature of the PW as well. In Fig. 1b we show the parametric evolution of the complex zeros in the $\mathcal{R}e(E) - \mathcal{I}m(E)$ -plane as the loss-strength γ increases. At the same figure we also mark with crosses the eigenvalues $\{E_n^{(0)}\}$ of the Hamiltonian H_0 . Initially (i.e. for $\gamma = 0$) the zeros are in the upper part of the complex plane (see blue and red circles) because of causality. As γ increases they move downwards and eventually cross the real axis at $E_{PW} \equiv E(k_{PW})$ corresponding to a critical value of $\gamma = \gamma_{PW}$. It is exactly this pair of (E_{PW}, γ_{PW}) for which a PW can be achieved. Notice that when $\mathcal{E} \ll 1$ (blue trajectories), the E_{PW} (whenever they exist) are very close to the eigenvalues $\{E_n^{(0)}\}$ of the isolated system. In the opposite limit of $\mathcal{E} \gg 1$, the PW energies E_{PW} occur between two nearby energy levels $\{E_n^{(0)}\}$ indicating that more than one mode might affect their formation.

Design schemes for WETACs –We start our analysis with the observation that a WETAC can be determined by a subset of the normalized eigenmodes $|\Psi_n^{(0)}\rangle$ of the Hamiltonian H_0 . The size \mathcal{N} of this subset depends on the Ericson parameter as $\mathcal{N} = [\mathcal{E}] + 1$, where $[\dots]$ indicates integer part. This reduced subspace is defined by a projection operator $P^{(\mathcal{N})} = \sum_{n=1}^{\mathcal{N}} |\Psi_{n_0+n}^{(0)}\rangle \langle \Psi_{n_0+n}^{(0)}|$

where $n_0 = 1, \dots, N - \mathcal{N}$.

Next, we project Eq. (6) in the $P^{(\mathcal{N})}$ subspace. The corresponding matrix elements of the reduced effective Hamiltonian $H_{eff}^{(\mathcal{N})}(-k, \gamma) = P^{(\mathcal{N})} H_{eff}(-k, \gamma) P^{(\mathcal{N})}$ are expressed in terms of the eigenvalues $\{E_n^{(0)}\}$ and eigenvectors $\{|\Psi_n^{(0)}\rangle\}$ of the isolated system i.e.

$$\begin{aligned} [H_{eff}^{(\mathcal{N})}(-k, \gamma)]_{nl} &= E_n^{(0)} \delta_{nl} - i\gamma \sum_d \langle \Psi_n^{(0)} | e_d \rangle \langle e_d | \Psi_l^{(0)} \rangle \\ &+ \frac{w^2 e^{-ik}}{t_L} \sum_m \langle \Psi_n^{(0)} | e_m \rangle \langle e_m | \Psi_l^{(0)} \rangle \end{aligned} \quad (7)$$

where the indexes d, m run over the position of the target(s) and the leads respectively. The potential WETAC pairs $(E_{WETAC}, \gamma_{WETAC})$ are associated with the real roots of the reduced secular equation $\zeta^{(\mathcal{N})}(E, \gamma) \equiv \det(H_{eff}^{(\mathcal{N})}(-k, \gamma) - E(k)) = 0$.

Out of all possible pairs $(E_{WETAC}, \gamma_{WETAC})$ which are solutions of the secular equation $\zeta^{(\mathcal{N})}(E, \gamma) = 0$ we consider only the ones that satisfy the following ‘‘proximity’’ constraints: (a) $E_{WETAC} \in [E_{min}^{(0)} - \delta, E_{max}^{(0)} + \delta]$ where $E_{min/max}^{(0)}$ are the borders of the energy interval associated with the eigenmodes of the reduced subspace $P^{(\mathcal{N})}$ and $\delta \ll \Delta$; and (b) the evaluated $\gamma_{WETAC} \in \bar{\gamma}[1 - \eta, 1 + \eta]$ where $\bar{\gamma}$ is the loss strength (conductivity) of the target and η is a tolerance level of our knowledge of its loss-strength. The corresponding subspace $P_{WETAC}^{(\mathcal{N})}$ which lead to a secular equation with solutions $(E_{WETAC}, \gamma_{WETAC})$ that satisfy the above two constraints constitute a good basis for the description of WETACs. The WETAC waveforms $|\mathcal{I}_{WETAC}\rangle$ correspond to the eigenvector $|\alpha_{max}^{(\mathcal{N})}\rangle$ associated with the maximum eigenvalue $\alpha_{max}^{(\mathcal{N})} = 1$ of the projected absorption operator $\mathcal{A}^{(\mathcal{N})}$. The latter is given by Eq. (4) with G substituted by $G^{(\mathcal{N})} \equiv P_{WETAC}^{(\mathcal{N})} G P_{WETAC}^{(\mathcal{N})}$.

Ergodic WETACs –In many practical situations, it is impossible to have information about the eigenmode amplitudes at the position of the target(s). We have therefore relax further the WETAC scheme by substituting in Eq. (7) for $H_{eff}^{(\mathcal{N})}$ (and consequently in $G^{(\mathcal{N})}$), the eigenmode amplitudes at the position of the target(s) with their ergodic limit i.e. $\langle e_d | \Psi_l^{(0)} \rangle \sim 1/\sqrt{N}$. This approximation is justified for chaotic cavities where typically the modes are ergodically distributed over the enclosure. We shall refer to this algorithm as the *ergodic WETAC*.

Below we test the proposed schemes for cavities with $\mathcal{E} \ll 1$ and $\mathcal{E} > 1$ as well as for cavities with and without TR-invariance.

Isolated Resonances – When $\mathcal{E} < 1$ the effective dimensionality of the projected subspaces is $\mathcal{N} = 1$ and thus $P_n^{(\mathcal{N}=1)} = |\Psi_n^{(0)}\rangle \langle \Psi_n^{(0)}|$ for $n = 1, \dots, N$. It turns

out that in this case the evaluation of $H_{eff}^{(\mathcal{N}=1)}$ requires only the knowledge of the field *intensities* at the position of the targets and at the position of the antennas, see Eq. (7). A potential pair $(E_{WETAC}, \gamma_{WETAC})$ is calculated from the reduced secular equation $\zeta^{(\mathcal{N})}(E, \gamma) = (\mathcal{Re}[\zeta^{(\mathcal{N})}], \mathcal{Im}[\zeta^{(\mathcal{N})}]) = (0, 0)$. The pair is accepted as a WETAC solution if it satisfies the proximity constraints mentioned above. In this case the subspace $P_n^{(\mathcal{N}=1)}$ is identified as $P_{WETAC}^{(\mathcal{N}=1)}$ and is used for the evaluation of the WETAC field via $\mathcal{A}^{(\mathcal{N}=1)}$. We get

$$|\mathcal{I}_{WETAC}\rangle \propto W^T |\Psi^{(0)}\rangle \quad (8)$$

where we have used Eq. (4) with the substitution of G with $G^{(\mathcal{N}=1)} = [|\langle \Psi^{(0)} | G | \Psi^{(0)} \rangle| |\Psi^{(0)}\rangle \langle \Psi^{(0)}|]$.

At Figs. 2a,b,c we show the numerical results for $\mathcal{P}(\alpha)$ (see staircase blue line) for $N_d = 1, 2, 4$ respectively. These distributions have been generated over a GOE ensemble of H_0 (for a fixed loss-strength $\tilde{\gamma}$) by substituting Eq. (8) together with the value of E_{WETAC} satisfying the proximity constraints, in Eq. (5) for the numerical evaluation of the absorbance.

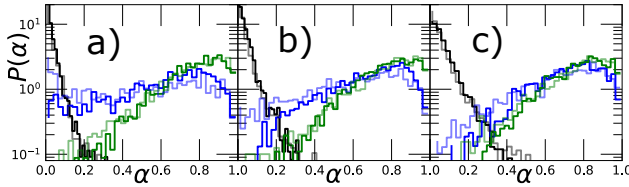


FIG. 3: (color online) Probabilities of absorbance $\mathcal{P}(\alpha)$ for a GOE/GUE cavities (dark/light lines) with $w = -1$ and $\mathcal{E} \approx 1.4/\mathcal{E} \approx 1.7$. (a) One lossy target; (b) two lossy targets; and (c) four lossy targets. The loss tolerance in all cases is $\eta = 0.3$. All other parameters are the same as in Fig. 2.

We proceed with the theoretical evaluation of $\mathcal{P}(\alpha)$. Using Eqs. (4,5) in the $P_{WETAC}^{(\mathcal{N}=1)}$ -space, we get the following expression for the absorbance

$$\alpha(k_{WETAC}, \tilde{\gamma}) = \frac{4\tilde{\gamma}\gamma_{WETAC}}{(\tilde{\gamma} + \gamma_{WETAC})^2}. \quad (9)$$

For simplicity, we assume that γ_{WETAC} is a gaussian random variable with the same mean and variance with the one associated with a box distribution $\tilde{\gamma}[1 - \eta, 1 + \eta]$. It is then straightforward to show that

$$\mathcal{P}(\alpha) \propto \sum_{\sigma=\pm} \frac{e^{-\frac{3}{2}(1-\alpha)(\frac{\alpha-\sigma}{\alpha\eta})^2}}{\sqrt{1-\alpha}(\alpha_\sigma - \alpha)} \quad (10)$$

where $\alpha_\sigma \equiv 2(1 + \sigma\sqrt{1-\alpha})$. The theoretical prediction Eq. (10) is plotted in Figs. 2a,b,c with a blue solid lines.

In Fig. 2 we also show the distribution of absorbances associated with incident waveforms $|\mathcal{I}_R\rangle = |\alpha_{max}(k)\rangle$ corresponding to eigenvectors of $\mathcal{A}(k, \tilde{\gamma})$ associated with

the maximum eigenvalue, and random wavevector taken from a box distribution in the interval $k \in [0, \pi]$. We find a fast decay of $\mathcal{P}(\alpha_{max})$ for large α indicating that majority of these waveforms will miss the lossy target, see staircase black line. Notice that any other random waveform will be much less efficient. In the same figure we also plot the theoretical results for $\mathcal{P}(\alpha_{max})$, see continuous black lines [30].

Let us now, analyze the efficiency of the ergodic WETAC scheme. An optimal impedance match condition implies that the WETAC pair $(E_{WETAC}, \gamma_{WETAC})$ must satisfy a flux-balance relation $\gamma_{WETAC} \sum_d |\langle e_d | \Psi_n^{(0)} \rangle|^2 \sim v_g \sum_m |\langle e_m | \Psi_n^{(0)} \rangle|^2$ where v_g is the group velocity at $E = E_{WETAC}$. This relation allows us to write $\gamma_{WETAC} = \tilde{\gamma}_{WETAC} \frac{N_d}{Y}$ where $Y \equiv N \sum_d |\langle e_d | \Psi_n^{(0)} \rangle|^2$ and $\tilde{\gamma}_{WETAC} = \gamma_{WETAC} \left| |\langle e_d | \Psi^{(0)} \rangle| \approx 1/\sqrt{N} \right.$. We interpret $\tilde{\gamma}_{WETAC}$ as the WETAC value for the loss-strength under the ergodic hypothesis for the field intensities at the position of the target(s) i.e. $|\langle e_d | \Psi^{(0)} \rangle| \approx 1/\sqrt{N}$. Then Eq. (9) for the absorbance is rewritten as

$$\alpha(k_{CPA}, \tilde{\gamma}) = \frac{4\tilde{\gamma}\tilde{\gamma}_{WETAC} \frac{N_d}{Y}}{(\tilde{\gamma} + \tilde{\gamma}_{WETAC} \frac{N_d}{Y})^2} \quad (11)$$

where now $\tilde{\gamma}_{WETAC} \in \tilde{\gamma}[1 - \eta, 1 + \eta]$. In the large- N limit, Y satisfies the generalized Porter-Thomas distribution $P_Y(y) \propto e^{-y/2} y^{N_d/2-1}$ while we can further assume that $\tilde{\gamma}_{WETAC}$ is an independent random variable that obeys a Gaussian distribution. Using Eq. (11) we get the distribution of the absorbances

$$\tilde{P}(\alpha) \propto \sum_{j=1,2} \frac{\alpha_j(1+\alpha_j)}{\alpha(1-\alpha_j)} I_j(N_d, \eta), \quad (12)$$

where $I_j(N_d, \eta) \equiv \int_0^\infty dx \exp\left[-\frac{3}{2\eta^2} \left(\frac{\alpha_j}{N_d}x - 1\right)^2 - \frac{x}{2}\right] x^{N_d/2}$

and $\alpha_j \equiv \left(2 - \alpha + (-1)^j 2\sqrt{1-\alpha}\right)/\alpha$. In Fig. 2 we plot with blue solid line the theoretical result Eq. (12) together with the numerical calculations (blue staircase line) for ergodic WETAC scheme. In comparison with the actual WETAC, the efficiency of the *ergodic WETAC* scheme to deliver the energy of the incident waveform at the lossy target is (obviously) reduced. The ergodic WETAC scheme is, nevertheless, far superior to the random incident waves (black lines). The level of efficiency is improved further when more lossy targets $N_d > 1$ are included in the complex enclosure, see Fig. 2b,c. The improvement is a direct consequence of the validation of the ergodic hypothesis in the limit of many targets $1 \ll N_d \ll N$.

Overlapping resonances – In this case the projected space is enlarged i.e. $\mathcal{N} > 1$. Below we consider the example case of $M = 2$ and $\mathcal{E} = 1.4$ corresponding to

$\mathcal{N} = 2$. The projection operator takes the form $P^{(\mathcal{N}=2)} = \left| \Psi_n^{(0)} \right\rangle \left\langle \Psi_n^{(0)} \right| + \left| \Psi_{n+1}^{(0)} \right\rangle \left\langle \Psi_{n+1}^{(0)} \right|$ for all subsequent modes $E_n^{(0)}, E_{n+1}^{(0)}$ of the isolated cavity H_0 . The potential WETAC pairs $(k_{WETAC}, \gamma_{WETAC})$ are obtained via Eqs. (6,7). Furthermore, the implementation of the proximity conditions allow us to single out the actual WETAC pairs and the corresponding WETAC subspaces $\mathcal{P}_{WETAC}^{(2)}$.

The design of the WETAC waveforms requires the diagonalization of the reduced absorption matrix $\mathcal{A}^{(\mathcal{N}=2)}$ in the WETAC subspaces $\mathcal{P}_{WETAC}^{(2)}$. The latter can be calculated using Eqs. (4, 7). The eigenvector $|\alpha_{\max}\rangle$ associated with the eigenvalue $\alpha = 1$ give us the desired WETAC $|\mathcal{I}_{WETAC}\rangle = |\alpha_{\max}\rangle$. For the case of one lossy target at position d_0 one has $|\mathcal{I}_{WETAC}\rangle \propto |u_{d_0}\rangle$ (see Eq. (4)), which in the $\mathcal{P}_{WETAC}^{(2)}$ space reads

$$|\mathcal{I}_{WETAC}\rangle \propto \left(\left[H_{eff}^{(\mathcal{N}=2)} \right]_{2,2} - E_{WETAC} \right) W^T \left| \Psi_1^{(0)} \right\rangle - \left[H_{eff}^{(\mathcal{N}=2)} \right]_{2,1} W^T \left| \Psi_2^{(0)} \right\rangle. \quad (13)$$

where $H_{eff}^{(\mathcal{N}=2)}$ has been evaluated at $(k_{WETAC}, \gamma_{WETAC})$, see Eq. (7). When $N_d > 1$ the incident waveforms $|\mathcal{I}_{WETAC}\rangle$ are evaluated numerically using the aforementioned WETAC algorithm. In Figs. 3a,b,c we report our numerical results for the distribution of absorbances $\mathcal{P}(\alpha)$ when a WETAC incident wave is launched towards the complex cavity (green staircase) with $N_d = 1, 2, 4$ lossy targets, respectively. At the same subfigures we report also the $\mathcal{P}(\alpha)$ associated with an ergodic WETAC (blue staircase). The two approaches converge rapidly to the same distribution as N_d increases. As a reference we also show the distribution $\mathcal{P}(\alpha)$ for the case of $|\mathcal{I}_R\rangle$ incident waveforms (black staircase).

WETACs for cavities with broken TR-invariance – In Fig. 3 we also report $\mathcal{P}(\alpha)$ for enclosures with broken TR-symmetry. The corresponding incident waveforms have been generated using the same WETAC scheme as above for $\mathcal{E} = 1.7$. We find that the WETAC (light green staircase) and the ergodic WETAC (light blue staircase) schemes demonstrate the same level of efficiency as in the GOE case. Light black staircase lines indicate the $\mathcal{P}(\alpha)$ generated from an ensemble of $|\mathcal{I}_R\rangle$ incident waveforms and it is shown for comparison.

Conclusions – We have proposed a statistical algorithm that allow us to design waveforms that deliver, with high probability, large portion of their energy in weakly lossy targets which are embedded inside chaotic enclosures. There are many open questions that need further investigation. For example, can we guarantee simultaneous multiple strikes? What is the effect of a weakly lossy background? How non-universal features (like scars) can be utilized for better performance? These questions will be the theme of future research in WETAC shaping.

Acknowledgments – We acknowledge influential discussions with Dr. A. Nachman who shaped the direction of this research activity. We thank Profs. S. Anlage, H. Cao and H. Schanz for useful discussions on WETAC design.

-
- [1] A. Mosk, A. Lagendijk, G. Lerosey, M. Fink, Nat. Phot. **6**, 283 (2012).
 - [2] P. Blomgeren, G. Papanicolaou, H. Zhao, J. Acoust. Soc. Am. **111**, 230 (2002).
 - [3] M. Fink, J. de Rosny, Nonlinearity **15**, R1 (2002).
 - [4] I. M. Vellekoop, A. Lagendijk, and A. P. Mosk, Nat. Photon. **4**, 320 (2010).
 - [5] E. G. van Putten, D. Akbulut, J. Bertolotti, W. L. Vos, A. Lagendijk, and A. P. Mosk Phys. Rev. Lett. **106**, 193905 (2011).
 - [6] O. Katz, E. Small, Y. Bromberg, Y. Silberberg, Nat. Photonics **5**, 372 (2011).
 - [7] Y. Choi, T. D. Yang, C. Fang-Yen, P. Kang, K. J. Lee, R. R. Dasari, M. S. Feld, W. Choi Phys. Rev. Lett. **107**, 023902 (2011).
 - [8] P. del Hougne, F. Lemoult, M. Fink, G. Lerosey, Phys. Rev. Lett. **117**, 134302 (2016).
 - [9] C. W. Hsu, S. F. Liew, A. Goetschy, H. Cao, A. D. Stone, Nat. Physics **13**, 497 (2017).
 - [10] M. Fink, D. Cassereau, A. Derode, C. Prada, P. Roux, M. Tanter, J.-L. Thomas, F. Wu, Rep. Prog. Phys. **63**, 1933 (2000)
 - [11] L. Borcea, G. Papanicolaou, C. Tsogka, J. Berryman, Inverse Probl. **18**, 1247 (2002).
 - [12] G. Montaldo, P. Roux, A. Derode, C. Negreira, M. Fink, Appl. Phys. Lett. **80**, 899 (2002).
 - [13] J. Dela Cruz, I. Pastirk, M. Comstock, V. Lozovoy, M. Dantus, Proc. Natl Acad. Sci. USA **101**, 17001 (2004).
 - [14] R. Horstmeyer, H. Ruan, C. Yang, Nat. Photonics **9**, 563 (2015).
 - [15] A. L. Moustakas, H. U. Baranger, L. Balents, A. M. Sengupta, S. H. Simon, Science **287**, 287 (2000).
 - [16] M. Davy, J. de Rosny, J.-C. Joly, M. Fink, C. R. Phys. **11**, 37 (2010).
 - [17] P. Ambichl, A. Brandstötter, J. Böhm, M. Kühmayer, U. Kuhl, S. Rotter, Phys. Rev. Lett. **119**, 033903 (2017)
 - [18] S. Rotter, S. Gigan, Rev. Mod. Phys. **89**, 015005 (2017).
 - [19] R. Holland and R. S. John, *Statistical Electromagnetics*, Taylor and Francis, and references therein.
 - [20] G. Gradoni, J.-H. Yeh, B. Xiao, T. M. Antonsen, S. M. Anlage, and E. Ott, Wave Motion **51**, 606 (2014).
 - [21] G. Tanner, N. Sondergaard, Journal of Physics A: Math. Theor. **40**, R443 (2007).
 - [22] M. Wright, R. Weaver, *New Directions in Linear Acoustics and Vibration*, University Press Cambridge, (2010).
 - [23] O. Legrand, D. Sornette, *Quantum chaos and Sabine's law of reverberation in ergodic rooms*, in *Large Scale Structures in Nonlinear Physics*, Lect. Notes Phys. **392** 267 (1991).
 - [24] G. Akemann, J. Baik, and P. Di Francesco, *The Oxford Handbook of Random Matrix Theory* (Oxford University Press, Oxford, 2010).
 - [25] H. J. Stockmann, *Quantum Chaos: An Introduction*, (Cambridge University Press, Cambridge, 1999).
 - [26] Y. D. Chong, L. Ge, H. Cao, A. D. Stone, Phys. Rev.

- Lett. **105**, 053901 (2010).
- [27] W. Wan, Y. Chong, L. Ge, H. Noh, A. D. Stone, H. Cao, Science **331**, 889-892 (2011).
 - [28] H. Li, S. Suwunnarat, R. Fleischmann, H. Schanz, T. Kottos, Phys. Rev. Lett. Vol. **118**, 044101 (2017)
 - [29] Y. V. Fyodorov, S. Suwunnarat, T. Kottos, J. Phys. A: Math. Theor. **50**, 30LT01 (2017).
 - [30] For a derivation of the theoretical formula see supplementary material.

SUPPLEMENTAL MATERIAL

We present here a theoretical analysis of the absorbance probability distribution $\mathcal{P}(\alpha)$ for the case that the incident waveforms are given by an ensemble of $|\mathcal{I}_R\rangle$ wavevectors (see main text). We restrict the discussion to the case of one loss target at site d_0 . From Eq. (4), we see that there is only one nonzero eigenvalue of the absorption matrix \mathcal{A} which is given as

$$\alpha = -4\gamma \frac{\sin k}{t_L} \langle u_{d_0} | u_{d_0} \rangle \approx -4\bar{\gamma} \frac{w^2}{t_L} \sum_m [H_0^{-1}]_{md_0}^2 \quad (14)$$

where we have assumed that the incident energy is in the middle of the band and the summation is over the number of leads $m = 1, \dots, M$.

Thus the study of the distribution $\mathcal{P}(\alpha)$ collapses to the study of the distribution of the statistically independent random variables $x = [H_0^{-1}]_{md_0}^2$, (H_0 is a GOE random matrix). Furthermore, one can show that for large values of x $\mathcal{P}(x) \sim 1/x^2$. In fact, numerical analysis indicates that the whole distribution can be nicely described by a Lorentzian i.e. $\mathcal{P}(x) = \frac{1}{\pi} \frac{x_0}{x^2 + x_0^2}$. Using this information in Eq. (14) we eventually get

$$\hat{P}(\alpha) \propto \int dx e^{ix \left(-\frac{\alpha t_L}{4\bar{\gamma} w^2} + M x_0^2 \right)} [\text{Erfc}(x_0 \sqrt{ix})]^M \quad (15)$$

where Erfc is the complementary error function.